中國機械工程學刊第四十卷第一期第 47~53 頁(民國一百零八年)
Journal of the Chinese Society of Mechanical Engineers, Vol.40, No.1, pp 47~53 (2019)

Thermal Analysis of Coupled Thermal Stress and Fatigue Life of a Diesel Engine Piston

Guang-Ju Xu*, Ming-Di Li**, Yang Zhao, Guang-Hua Li and Qing-Zhang Chen

Keywords： diesel engine; piston; heat load; fatigue life; finite element.

ABSTRACT

Using PERMAS software, the temperature and thermal-mechanical coupled stress of a piston under calibration conditions were calculated using the finite element model for the piston skirt profile, the piston combustion chamber and the inner cooling oil path. The fatigue life of the piston was analyzed, and the changes in the piston ring groove and the outer diameter of the piston were measured. The results show that the high temperature region of the piston is mainly distributed at the top of the piston and that the maximum temperature is approximately 301 ℃, which is within the allowable range of the piston material; the average surface temperature of the first ring groove is 194 ℃, which is lower than the lubricating oil coking temperature. When the piston is coupled to a heat engine, the piston is tilted toward the main thrust surface, and the main thrust surface is larger, approximately 44 N / mm^2. The maximum stress value of the piston pin seat surface is mainly distributed in the back pin hole, and the stress values are within the allowable range. The lowest fatigue life of the piston occurs at the bottom part of the combustion chamber and the combustion chamber roar mouth, which have theoretical fatigue lives of 6.9 and 7.7, respectively. After 800 hours of thermal shock testing, the piston ring groove, pin hole, piston ring groove bottom diameter and the piston show little change in dimension. All of these piston elements meet the fatigue life requirements.

Paper Received, November, 2016. Revised March, 2017. Accepted April, 2017. Author for Correspondence: Ming-Di Li.

* *Associate Professor, School of Automotive Engineering, Changshu Institute of Technology,Changshu 215500,CHINA*

** *lecturer，School of Automotive Engineering, Changshu Institute of Technology,Changshu 215500,CHINA*

INTRODUCTION

Pistons are one of the most important components of diesel engines, along with the connecting rods, crankshaft and other connecting mechanisms. The reciprocating motion of the piston produces rotary motion output [1-5]. During this process in the diesel engine, the piston is subjected to periodic mechanical loads, such as inertial forces, lateral pressures and friction forces generated by the high-speed reciprocating motion . On the other hand, because of the high temperature and high pressure gas produced during the combustion process, the surface temperature varies among the different parts of the piston. As the temperature gradient increases, the temperature distribution becomes uneven, leading to increased thermal stresses and thermal deformation of the piston. With increasingly stringent emission regulations, continuous improvement of the diesel engine working pressures is needed. With the upgrade from the country Ⅲ to the country Ⅳ emissions standard, the maximum cylinder outbreak pressure increased by approximately 13%, and the rate of the rapid combustion cylinder pressure increased to 0.6 ~ 0.8 MPa / ° CA [6-8]. Due to excessive thermal stress and thermal deformation of the piston from large unequal heating, piston surface cracking, perforations and other failures could occur [9-11]. Comprehensive diesel piston calculations are necessary to improve the reliability of the piston and to extend the life of the piston. The PERMAS software was used to optimize the piston and combustion chamber, with its internal cooling oil channel, by calculating the temperature fields of the piston, the piston skirt profile and the pin hole profile under optimized conditions. The fatigue life of the piston was analyzed, and the piston was subjected to a thermal shock test for 800 hours. The fatigue life of the piston was measured by thermal shock testing, and the fatigue life of the piston was analyzed. Measurements of the piston ring groove, pin hole, piston ring groove bottom diameter and piston dimensions and their profile changes were obtained.

ESTABLISHING THE PISTON FINITE ELEMENT MODEL

Modeling and meshing

In view of the increased pressure inside the cylinder and the increased temperatures of the gases at the top of the piston, the shape and position of the cold oil path in the piston were optimized. The head and the combustion chamber cooling became more effective after these improvements. As shown in Fig. 1, the solid line represents the combustion chamber with the inner cooling channel before improvement, and the dotted line represents the optimized combustion chamber with the internal cooling oil channel. The position of the optimized internal cooling channel was improved when the distribution channel was added. In addition, the optimization further improved the cooling of the piston combustion chamber at the bottom of the piston and the head.

Fig 1. Piston cooling oil passage before and after optimization schematic

The piston finite element model includes the connecting rod, piston, piston-pin and cylinder liner. In the three-dimensional model of the piston group, considering that the piston pin bias is not fully symmetrical, using Pro-E software was used for the piston skirt profile, pin hole profile, piston optimization of the combustion chamber and internal cooling oil. By modeling the piston of the card spring slot, the oil return hole was simplified. The piston model used HyperMesh software. As shown in Fig. 2, the piston, ring and connecting rod adopted the second-order tetrahedral mesh. The piston pin and cylinder liner adopted the first-order reduction hexahedral mesh. The number of piston nodes was 801575, and the number of units was 509476.

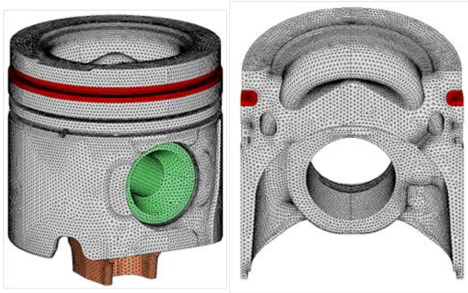

(a) Overall view (b) Sectional view

Fig 2. Piston grid

Setting the boundary conditions

Pistons operating within a diesel engine must withstand the forces of gas combustion pressures generated by the reciprocating motion of the piston, the inertial forces generated by the piston and the cylinder liner friction forces. The cylinder sleeve and piston skirt also generate pressures due to the interaction of the side pressure[12、13]. The explosion pressures, applied forces and piston deformations are highest in a diesel engine under calibration conditions. Therefore, it is key to study the mechanical strength of the pistons with these conditions under mechanical loads.

Thermal boundary conditions

Accurate thermal boundary conditions of the piston are important for simulating the temperature field with the finite element model. The maximum thermal load condition was defined for the calibration case, using the third type of thermal boundary conditions provided previously[14-16]. The measured piston temperature of the diesel engine was taken as the heat load input condition, as shown in Table 1.

Table 1. Piston temperature results

No	Position	The first cylinder temperature (℃)	The third cylinder tmperature (℃)	The fifth cylinder temperature (℃)
1	Combustor center	260	248	244
2	Open combustion chamber	310	288	280
3	The bottom of combustion chamber	217	211	226
4	The first ring	238	234	233
5	The front end of the pin hole	188	165	178
6	The rear end of the pin hole	188	189	180

Among the piston temperatures, the maximum piston temperature (310 ℃) was located in the combustion chamber mouth, and the lowest temperature zone was located in the front pin hole (165 ℃). The temperature field distribution of the piston was reasonable and satisfied the requirements of the finite element boundary conditions. The temperature field distribution was calculated for the oil chamber of the upright ring, the oil hole in the two pin, from the cooling nozzle high-speed injection into the oil chamber and then the oil hole, and for the piston reciprocating motion from the oil hole after the return oil. In this process, the bottom shell had good heat transfer properties. Using empirical data from the test tube, the following empirical formula was used for the internal cooling cavity calculation:

$$Nu_t = 0.495\,\mathrm{Re}_t^{0.57}\,D^{*0.24}\,\mathrm{Pr}_t^{0.29} \tag{1}$$

$$Nu_t = \frac{\alpha D}{\gamma} \tag{2}$$

$$D^* = \frac{D}{b} \tag{3}$$

$$\mathrm{Re}_t = \frac{uD}{\upsilon_t} \tag{4}$$

In the formula, Nut is the Nusselt criterion number, Ret is the Reynolds number of the lubricating oil flow, Prt is the Prandtl number, α is the heat transfer coefficient, D is the equivalent diameter of the cooling oil chamber, γ is the lubricating oil thermal conductivity, B is the average height of the cooling oil chamber, u is the lubricating oil speed and νt is the lubricating oil kinematic Viscosity. and table 2 was the data of engineering materials.

Table 2. Data of engineering materials

No	Material properties	Parameter
1	density（kg/dm^3）	2.7
2	Elastic modulus（N/mm^2）	84000
3	Poisson ratio（μ）	0.32
4	Thermal expansion coefficient（1/K）	19.2×10^{-6}
5	Piston ring elastic modulus（N/mm^2）	110000
6	Piston pin elastic modulus（N/mm^2）	207000

Piston mechanical load

The mechanical load on the piston mainly comes from the gas pressure, inertial forces and lateral forces. Fig. 3 shows the in-cylinder burst pressure and lateral pressure changes that the piston is able to withstand with the crank angle relationship. The gas pressure on the top surface of the piston was treated as a uniform load, wherein the top surface of the piston, the upper and lower side surfaces of the first ring groove and the piston fire are loaded according to the maximum burst pressure. The first ring and the second groove had the largest burst pressure (20% of the load). When the load was ignored, the uniform pressure was not applied on the second ring groove, taking into account the gas pressure. Piston loads when applying side pressures in the piston and cylinder liner contact surface are not evenly distributed, and the space between the piston skirt incurred the maximum lateral pressure. The piston lateral pressure was approximated for the piston circumference, the piston and the cylinder liner. Using the law of the internal force distribution and the law of cosines, the pressure curve of the oil film in the direction of the force and the direction of the piston axis and side pressure formed a parabolic secondary distribution[17].

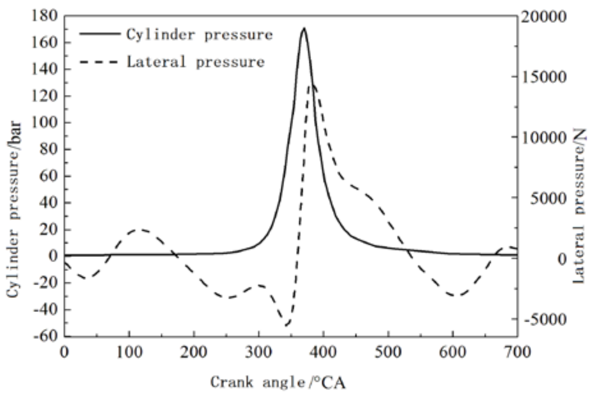

Fig 3. In-cylinder combustion pressure and lateral pressure curve

TEST EQUIPMENT AND PROGRAMS

The diesel thermal shock equipment is composed of a multi-stage circulating pump, heat exchanger, cold water tank, hot water tank, and a hot and cold shock control unit. The thermal shock test process of a diesel engine can be tested using this setup. To determine the optimum cold and hot cycle times, a cylinder head calibration test was performed prior to the thermal shock test.

The thermal shock test cycle time was determined by installing the temperature sensor in the cylinder head valve nose bridge area. Then, the calibrated cylinder head was installed on the diesel engine to calibrate the thermal shock test cycle time and to obtain the metal temperature of the cylinder head. According to the results of the cylinder head calibration, the thermal shock test cycle time was 360 s, including cycles of 195 s, 135 s and 30 s. For the thermal cycle conditions, the diesel engine running at the calibration speed required 100 ℃ water. For the low temperature cold cycle at low idle speed conditions, the water temperature was 30 ℃. A thermal shock test was carried out for 8,000 cycles for a total of 800 hours.

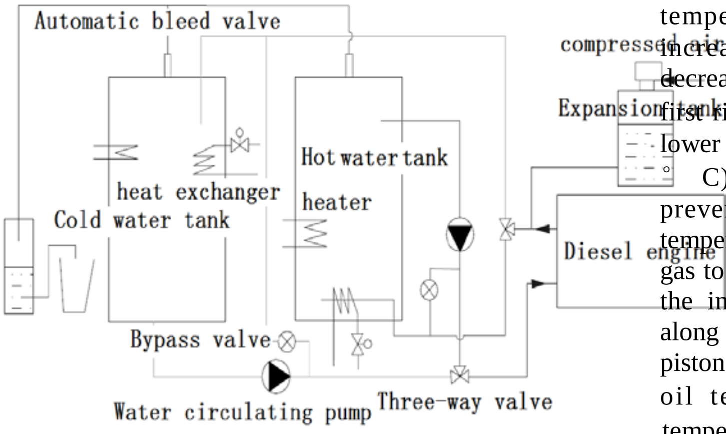

Fig 4. Thermal shock device schematic

RESULTS ANALYSIS AND DISCUSSION

Piston temperature field

When calculating the temperature field of the piston, it is necessary to give a reasonable heat transfer boundary condition, which is the key condition for the finite element calculation. The finite element software was used to calculate the temperature field of the piston for comparison with the actual temperature measured at each point. In Fig. 5, the left side of the figure is the measured value, and the right side is the calculated value. The measured temperature agreed well with the calculated value; the maximum temperature deviation was approximately 4 ℃, and had good regularity, which shows that the heat transfer boundary condition was reasonable and that the model was accurate

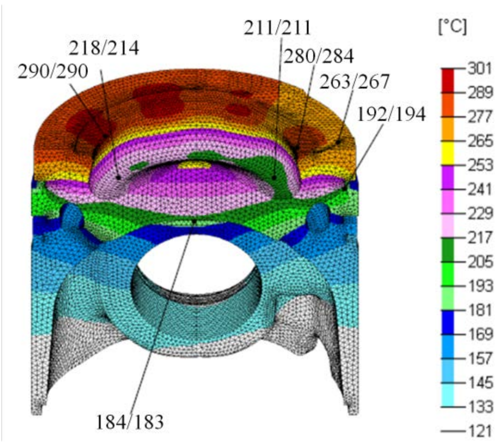

Fig 5. Comparison of piston temperature field calculation and measured values

As shown in Fig. 5, the piston circumference temperature distribution was more uniform than the cylinder piston temperature distribution in the axial direction. The high temperature distribution at the top of the piston was approximately 301 ℃, which was lower than the aluminum alloy piston heat temperature (360 ℃). The piston head radius increased as the surface temperature gradually decreased. The average surface temperature of the first ring groove of the piston was 194 ℃, which is lower than the lubricating oil coking temperature (230 C). Hence, the average surface temperature prevented coking of the lubricating oil at high temperature. Since most of the heat transferred by the gas to the piston mainly relied on the piston ring and the internal cooling oil chamber, the temperature along the axial direction from the piston top to the piston skirt gradually decreased. The internal cooling oil temperature was 220 ℃, and the upper temperature of the pin hole was 183℃.

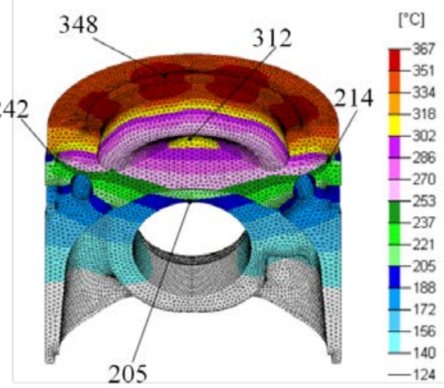

Fig 6. After a 20% increase in the amount of fuel injection piston surface temperature

Studies have shown that excessive fuel injection caused by the wear of the injector can lead to piston cracking. Based on the piston temperature measurement results, the temperature distribution of the piston surface was calculated when the injection quantity was increased by 20%, as shown in Fig. 6. The surface temperature distribution of the piston was almost the same with and without increasing the injection quantity. The maximum temperature of the piston surface was approximately 348 ℃. The average surface temperature of the first ring groove of the piston was 214 ℃. The temperature of the internal cooling oil channel and rear pin and that of the upper side of the hole were 242 ℃ and 205 ℃,respectively. This indicates that the surface temperature of the piston was improved within the permissible range of the piston material when subjected to the heat load, which meets the design requirements. Thus, the piston can work normally when excessive oil is injected.

Coupled thermal-mechanical stress on the piston

Based on the heat load and mechanical load, the highest combustion pressure was applied to obtain the stress and deformation of the piston under the coupled load of the heat engine [18-21]. The piston temperature field was increased with 20% as the thermal boundary input, taking into account the inertial force, the cylinder gas pressure and the maximum lateral pressure. The stress distribution of the piston under the heat engine load is shown in Fig. 7. Under the highest combustion pressure, the piston was tilted toward the main thrust surface, and the main thrust surface of the piston was strong. The average stress was approximately 44 N / mm^2, which was within the allowable range. The maximum stress value of the surface of the piston pin seat surface was mainly distributed on the upper side of the rear pin hole and was approximately 98 N / mm^2, which was mainly due to the full constraints of the lower end of the connecting rod caused by the piston pin. The piston pin contact stress value was higher than the actual engine operating state value, but the stress values were within the allowable range for the materials used and were in line with the design requirements.

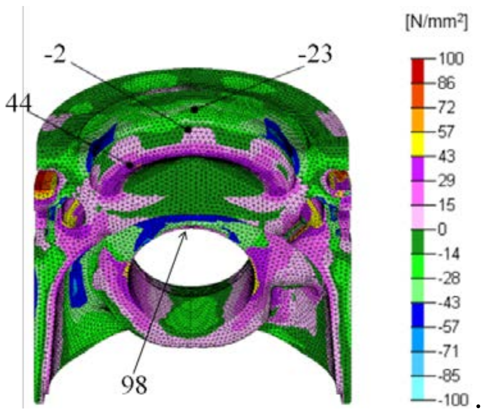

Fig 7. Pistons mean stress

Piston fatigue life analysis

The thermal fatigue of the piston materials was analyzed, which included thermal strain cycles. The thermal strain needs to be considered given the high gas temperatures in the cylinders and the changing temperature effects. Diesel engines frequently have multiple start-stop operations. When these thermal strains are large, they can cause serious damage to the piston. Piston damage is attributed to high cycle fatigue (HCF), low cycle fatigue (LCF), and thermo-mechanical fatigue (TMF). During the simulation analysis, the load spectrums of the piston were accumulated, as shown in Fig. 8. The piston test run-time, cumulative damage ratio, piston life evaluation index and piston fatigue life analysis are shown.

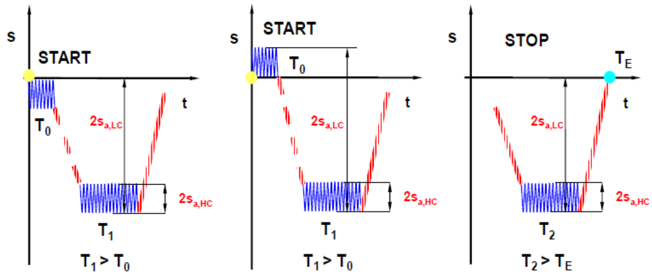

Temperature and material characteristics of the piston

Adiabatic process

（a）T1>T0　（b）T1>T0　（c）T2>TE

Fig 8. Piston Life Calculation

Fig. 9 shows the calculated fatigue life for various parts of the piston. The lowest fatigue life of the piston occurred at the bottom of the combustion chamber and the combustion chamber roar mouth. The theoretical fatigue life values of these parts were 6.9 and 7.7, respectively. Although the piston throat and the bottom of the combustion chamber were the weakest parts of the piston, their fatigue lives were greater than 2.5, which meets the needs of diesel engines.

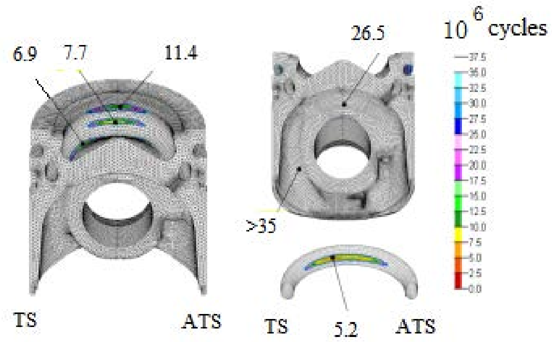

Fig 9. Various parts of the piston fatigue life prediction

To further analyze the fatigue life of the piston after optimization, the piston was analyzed with 800 hours of thermal shock testing, and the piston did show cracking, perforation or other failures. The piston cavity did not overheat. The thermal shock test measured the piston ring groove, pin hole, piston ring groove bottom diameter, and piston outer diameter, as shown in Table 3. The maximum wear of the first ring groove width was 0.006 mm. The first ring groove bottom diameter was not worn. The maximum wear of the second ring groove width was 0.008 mm. The maximum wear of the second ring groove bottom diameter was 0.01 mm. The maximum wear of the oil ring groove was 0.002 mm. The maximum wear of the oil ring groove bottom diameter was 0.005 mm. The maximum outer diameter of the piston was not worn. The maximum wear of the piston pin hole was 0.013 mm. The oval-shaped lines of the cylindrical piston were normal. The results show that the optimized piston had better fatigue resistance and better reliability.

Table 3. The abrasion of piston measurement results

Measuring position	Maximum wear/mm
The first ring groove width	0.006
Root diameter of the first ring	0
The second gas ring width	0.008
Root diameter of the second rings	0.010
Oil ring groove width	0.002
Oil ring groove bottom diameter	0.005
Piston outer diameter	0
Piston pin hole	0.013

CONCLUSIONS

(1) The temperature distribution in the circumference of the piston was relatively uniform. The piston temperature distribution in the axial direction of the cylinder was quite different, and the high temperature region was located at the top of the piston. The maximum temperature was approximately 301 ℃; this is within the permissible range for the piston material. The average surface temperature was 194 ℃, which was lower than the lubricating oil coking temperature of 230 ℃. Thus, this temperature will avoid the high oil temperatures produced by the coking phenomenon. Therefore, the fuel injection can be increased by 20%, and the piston surface temperature meets the design requirements.

(2) When the piston was exposed to the engine heat, the piston was inclined toward the main thrust surface, and the force was approximately 44 N / mm^2. The area with the maximum stress was mainly distributed on the upper side of the piston pin, which was approximately 98 N / mm^2. Both of these stress values are within the allowable range.

(3) The fatigue life of the piston was lowest at the bottom of the piston chamber and the combustion chamber, which had theoretical fatigue lives of 6.9 and 7.7, respectively. The fatigue life of the weakest piston components was more than 2.5, which meets the requirements for diesel engines. After 800 hours of thermal shock testing, the pistons showed no cracking. The piston and the piston cavity did not show any other defects due to overheating. The piston ring groove, pin hole, piston ring groove bottom diameter, and the piston showed little changes in their outer diameter dimensions. The cylindrical and elliptical piston lines also showed little changes. Thus, all the piston elements meet the fatigue life requirements.

ACKNOWLEDGMENT

The authors gratefully acknowledge financial support from National Natural Science Foundation of China (NSFC. 51506011,11802039), Natural Science Foundation of Jiangsu Province (BK20160406), Natural Science Research Project of Jiangsu Higher Education Institutions (15KJB470001,18KJB470001) and Basic research project of Suzhou (SYG201515).

REFERENCES

Zhang W Z, Wei C Y, Su Z G, et al. A study on forecasting of fatigue life for aluminium alloy piston of diesel engine [J]. China Mechanical Engineering, 2003, 14(10): 865-867.

Zhang W X, Gao G D, Mu G Y. Surplus Fatigue Life Prediction of Diesel Engine Piston by the Equivalent J-Integral Approach[J]. Advanced Materials Research, 2011, 399-401:2305-2308.

Lu X，Li Q，Zhang W，et al. Thermal analysis on piston of marine diesel engine [J]. Applied Thermal Engineering, 2013, 50(1):168-176.

Lei J L, Shen L Z, Yang Y Z, et al. Finite element analysis and temperature field measurement of 4100QBZ turbo charged diesel engine piston [J]. Transactions of CSICE, 2007, 25(5): 445-450.

Sharma S K, Saini P K, Samria N K. Experimental Thermal Analysis of Diesel Engine Piston and Cylinder Wall[J]. Journal of Engineering, 2015, 2015:1-10.

Cerit M. Thermo mechanical analysis of a partially ceramic coated piston used in an SI engine[J]. Surface and Coatings Technology, 2011, 205(11):3499-3505.

Tamminen J, Sandström C E, Andersson P. Influence of load on the tribological conditions in piston ring and cylinder liner contacts in a medium-speed diesel engine[J]. Tribology International, 2006, 39(12):1643-1652.

Zu B F, Fang Q, Liu J, et al. Numerical analysis of piston strength and deformation based on Thermo-mechanical coupling for China－V diesel engine[J].Chinese Internal Combustion Engine Engineering. 2014, 35(1):99-104.

Zhang J H, He Z P, Zhang G C, et al. Coupled thermal and Mechanical Load Analysis in Diesel Engine Piston[J]. Transactions of CSICE, 2011, 29(1):78-83.

Sung S J, Wook H Y, Sung C A, et al. Design and application of composite pistion for high power diesel engine[C]. SAE 2009-01-0192, 2009.

Mohamad S A, Lu X, Zheng Q. Numerical modeling of lubrication of piston ring of two-stroke marine diesel engine considering the effect of multi-scale grooves on the cylinder liner[J]. Proceedings of the Institution of Mechanical Engineers Part J Journal of Engineering Tribology, 2015, 229(8):989-1002.

Söchting S J, Sherrington I. The effect of load and viscosity on the minimum operating oil film thickness of piston-rings in internal combustion engines[J]. ARCHIVE Proceedings of the Institution of Mechanical Engineers Part J Journal of Engineering Tribology 1994-1996 (vols 208-210), 2009, 223(223):383-391.

M.P.Rodriguez, N.Y.A.Shammas. Finite element simulation of thermal fatigue in multiplayer and structures: thermal and mechanical approach[J]. Microelectronics Reliability. 2001.Vol.41.Issue584:517-523.

Huaqiang Chu, Weiwei Han, Wenjian Cao, et al.Effect of methane addition to ethylene on the morphology and size distribution of soot in a laminar co-flow diffusion flame[J], Energy, 2019,166（1）:392-400.

Andreas P, Harold S, Boon K C, et al. Parameterization and FEA approach for the assessment of position characteristics[C]. SAE 2006-01-0429, 2006.

Woshni G,Fieger J.Determination of local heat transfer coefficients at the piston of a high speed diesel engine by evaluation of measured temperature distribution，SAE Paper 790834，1979

Li Y. Simulation and application of solid-liquid coupled heat transfer in internal combustion engines[D].Zhejiang university, 2006.

Liu Q, Ouyang G Y, Zhang P. Three-Dimensional Finite Element Coupled Analysis of a Diesel Engine Piston[J]. Applied Mechanics & Materials, 2014, 684:347-353.

Wang Y, Liu Y, Shi H. The Reliability Analysis for Pistons on Fracture Mechanics[C]// International Conference on Computer Modeling and Simulation. IEEE, 2010:173-177.

Liu Z M, Li C, Hou X Q. Analysis of Thermal-Mechanical Coupling Strength and Fatigue Life of Piston of Low Speed Diesel Engine[J]. Advanced Materials Research, 2012, 562-564:560-563.

Hoeppner DW. Fretting Fatigue Case Studies of Engineering Contents[J]. TribologyInternational, 2006, (10):1271-1276

基於熱機耦合的柴油機活塞熱應力與疲勞壽命分析

許廣舉 李銘迪 趙洋 李廣華 陳慶樟
常熟理工學院汽車工程學院

摘 要

本文通過建立活塞裙部型線、活塞優化後的燃燒室及內冷油道等的有限元模型，採用 PERMAS 軟體，計算了優化後的活塞在標定工況下的溫度場和熱機耦合應力，分析了活塞的疲勞壽命，並測量了 800 小時熱衝擊試驗後，活塞環槽、活塞外圓尺寸等尺寸和型線的變化情況。結果表明，活塞高溫區域主要分佈在活塞頂部，最高溫度約為 301℃，在活塞材料許用範圍內；第一環槽的表面平均溫度為 194℃，低於潤滑油結焦溫度 230℃，增加 20%噴油量時，活塞的表面溫度仍可滿足設計要求。在活塞受到熱機耦合作用時，活塞向主推力面方向傾斜，主推力面受力較大，約為 44N/mm2，活塞銷座表面最大應力值區域主要分佈在後端銷孔上側，約為 98 N/mm2，應力值均在許用範圍內。活塞疲勞壽命最低的部位在活塞燃燒室底部及燃燒室吼口，理論壽命分別為 6.9 和 7.7，800 小時熱衝擊試驗後，活塞環槽、銷孔、活塞環槽底徑、活塞外援尺寸等尺寸變化均較小，活塞外圓型線和橢圓型線變化不大，能夠滿足使用要求。